
Article:
Li, N., Oakes, J.A., Storbeck, K.-H. et al. (2 more authors) (2020) The P450 side chain cleavage enzyme Cyp11a2 facilitates steroidogenesis in zebrafish. Journal of Endocrinology, 244 (2). pp. 309-321. ISSN 0022-0795

https://doi.org/10.1530/joe-19-0384

The P450 side chain cleavage enzyme Cyp11a2 facilitates steroidogenesis in zebrafish

Nan Li[1, 2], James A Oakes[1, 2], Karl-Heinz Storbeck[3], Vincent T Cunliffe[2, 4#], Nils P Krone[1, 2, 5#].

[1] Department of Oncology & Metabolism, School of Medicine, University of Sheffield, Sheffield, S10 2TH, United Kingdom
[2] The Bateson Centre, Firth Court, Western Bank, Sheffield, S10 2TN, United Kingdom
[3] Department of Biochemistry, Stellenbosch University, Stellenbosch, 7602, Matieland, South Africa
[4] Department of Biomedical Science, Firth Court, Western Bank, Sheffield, S10 2TN, United Kingdom
[5] Department of Medicine III, University Hospital Carl Gustav Carus, Technische Universität Dresden, 01307 Dresden, Germany

Short title for page heading: Cyp11a2 and steroidogenesis in zebrafish

Key words: Cyp11a2, glucocorticoid, androgen, zebrafish, CRISPR/Cas9

Word count: 5,243

[#]VCT and NPK contributed equally to the work.

Corresponding author / reprint requests:

Nils P Krone MD FRCPCH
Academic Unit of Child Health
Department of Oncology & Metabolism
University of Sheffield
Sheffield Children's Hospital
Western Bank
SHEFFIELD S10 2TH
UNITED KINGDOM

Email: n.krone@sheffield.ac.uk

Disclosure Summary: Nothing to disclose.

Abstract

Cytochrome P450 side-chain cleavage enzyme, encoded by the *CYP11A1* gene, catalyzes the first and rate-limiting step of steroid hormone biosynthesis. Previous morpholino knockdown studies in zebrafish suggested *cyp11a2* is a functional equivalent of human *CYP11A1* and is essential for interrenal steroidogenesis in zebrafish larvae. The role of Cyp11a2 in adult zebrafish, particularly in gonadal steroidogenesis, remains elusive. To explore the role of Cyp11a2 in adults, we developed zebrafish mutant lines by creating deletions in *cyp11a2* using the CRISPR/Cas9 genomic engineering approach. Homozygous *cyp11a2* mutant zebrafish larvae showed an upregulation of the hypothalamic–pituitary–interrenal axis. Furthermore, these Cyp11a2-deficient zebrafish demonstrated profound glucocorticoid and androgen deficiencies. *Cyp11a2* homozygotes only developed into males with feminized secondary sex characteristics. Adult *cyp11a2*$^{-/-}$ mutant fish showed a lack of natural breeding behaviors. Histological characterization revealed disorganized testicular structure and significantly decreased numbers of mature spermatozoa. These findings are further supported by the downregulation of the expression of several pro-male genes in the testes of *cyp11a2* homozygous zebrafish, including *sox9a*, *dmrt1* and *amh*. Moreover, the spermatogonia markers *nanos2* and *piwil1* were upregulated, while the spermatocytes marker *sycp3* and spermatids marker *odf3b* were downregulated in the testes of *cyp11a2* homozygous mutants. Our expression analysis is consistent with our histological studies, suggesting that spermatogonia are the predominant cell types in the testes of *cyp11a2* homozygous mutants. Our work thus demonstrates the crucial role of Cyp11a2 in interrenal and gonadal steroidogenesis in zebrafish larvae and adults.

Introduction

Zebrafish has been established as vertebrate model to elucidate gene function in development and disease. Despite their evolutionary distances, zebrafish share extensive conservation with humans at both genomic and functional levels. In particular, molecular pathways controlling steroidogenesis and steroid signaling are highly conserved (Lohr and Hammerschmidt, 2011, Tokarz *et al.*, 2013, Tokarz *et al.*, 2015). Similar to humans, cortisol is the main glucocorticoid in zebrafish and is produced in the interrenal (equivalent of the mammalian adrenal gland) (Dickmeis, 2009). The production of cortisol is under the control of hypothalamus and pituitary, forming the hypothalamus-pituitary-interrenal (HPI) axis (Liu, 2007, To *et al.*, 2007). In addition to the interrenal, steroidogenesis in zebrafish also occurs in other tissues such as gonads and brain (Tokarz *et al.*, 2013).

The cytochrome P450 side-chain cleavage enzyme, encoded by the *CYP11A1* gene, catalyzes the first and rate-limiting step of steroidogenesis and is a prerequisite for all steroid biosynthesis (Miller and Auchus, 2011). Previous studies identified two *cyp11a* genes in zebrafish, *cyp11a1* and *cyp11a2* (Goldstone *et al.*, 2010, Parajes *et al.*, 2013). Our previous work assumed a paralog-specific role for each *cyp11a* gene in zebrafish larvae (Parajes *et al.*, 2013). During early development, *cyp11a1* is expressed from zygote to segmentation periods (22-24hpf, hours post fertilization) while the expression of *cyp11a2* becomes prominent just before the onset of *de novo* (48hpf) and HPI-mediated (96hpf) cortisol biosynthesis. Morpholino-mediated mRNA knockdown revealed that *cyp11a1* is required for early embryonic development, whereas its paralog *cyp11a2* represents the functional equivalent of human *CYP11A1* and is essential for interrenal steroidogenesis in larvae (Parajes *et al.*, 2013).

However, loss-of-function studies using morpholinos only transiently reduce expression levels of target genes, and the physiological role of Cyp11a2 in adult zebrafish remains unclear. To define the function of Cyp11a2 in adult zebrafish, we developed zebrafish *cyp11a2* null alleles using a CRISPR/Cas9 approach. Cyp11a2-deficient zebrafish had a phenotype resembling severe combined interrenal and gonadal insufficiency, including decreased expression of glucocorticoid target genes, altered steroid hormone profiles, reduced fertility, disorganized gonadal tissues and all-male fish with feminized secondary sex characteristics. Thus, we demonstrate that *cyp11a2* is the functional P450 side-chain cleavage enzyme paralog in zebrafish, facilitating the primary step of interrenal and gonadal steroidogenesis.

Material and methods

Zebrafish maintenance

The zebrafish strains were maintained in a recirculating system (ZebTECTM, Techniplast®, Kettering, UK and Sheffield, UK) at 28.5°C in a 10-hour dark, 14-hour light photoperiod. Embryos were obtained by natural spawning and incubated at 28.5°C in E3 medium (5mmol/L NaCl, 0.17mmol/L KCl, 0.33mmol/L CaCl2, 0.33mmol/L MgSO4) containing 0.1% (v/v) methylene blue. The developmental stages were determined according to hours post fertilization (hpf), and days post fertilization (dpf). All procedures were approved by the United Kingdom Home Office and carried out in line with the Animals (Scientific Procedures) Act 1986.

Generation of *cyp11a2* mutants by CRISPR/Cas9

Gene-specific guide RNA (gRNA) was designed against an optimal CRISPR site targeting exon 5 of *cyp11a2* (ENSDARG00000092696) following an adapted strategy described previously (Hruscha *et al.*, 2013, Talbot and Amacher, 2014). gRNA antisense DNA sequence was first amplified using 2.5µl gRNA primer 1 (10µM, 5'-GCGTAATACGACTCACTATAG-3'), 2.5µl gRNA primer 2 (10µM, 5'-AAAAAAGCACCGACTCGGTGCCAC-3'), 2µl gRNA guide oligo (1µM, oligonucleotide sequence is listed in Supplementary Table 1), 20µl 5x FIREPol® Master Mix (Solis Biodyne, Tartu, Estonia), and 73µl MilliQ H_2O. The whole PCR product was loaded on a 2.5% (w/v) agarose gel and extracted using MinElute Gel Extraction Kit (Qiagen, Venlo, Netherlands) following the manufacturer's protocol. The subsequent *in vitro* transcription was performed using MEGAshortscript T7 kit (Life Technologies, California, USA), using 1µl as a template. Fertilized eggs were injected at 1-cell stage with 1nl of a solution containing 2µM Cas9 protein (NEB, Herts, UK), 2.4ng/nl gRNA and 0.1% (v/v)

131 phenol red. Genomic DNA was extracted from injected individuals at 5dpf to
132 verify the presence of mutations and confirm the activity of the gRNA. Injected
133 embryos were raised to adulthood (F0 generation). To confirm germline
134 transmission of the mutation, a pool of 20 embryos collected from out-crosses
135 between the F0 and wild-type were genotyped. F0 fish with successful germline
136 transmission were kept as F0 founders. Embryos from out-crosses were raised
137 to generate the F1 generation and genotyped for heterozygous mutations using
138 fin clips. F1 heterozygotes were then out-crossed to generate the F2
139 heterozygotes which were in-crossed to characterise the *cyp11a2* mutations.
140

141 **Genotyping *cyp11a2* mutants**

142 Adult fish were anesthetized in tricaine methanesulfonate (MS222, Sigma-
143 Aldrich, Missouri, USA) and one-third of caudal fin was cut with a sharp blade.
144 Genomic DNA was extracted from clipped caudal fin tissue or from whole
145 larvae. Samples were lysed in 20µl of 50mM NaOH and boiled for 10 minutes
146 at 98°C and 1/10 volume of 100mM Tris-HCl pH8.0 was added to buffer the
147 reaction. PCR amplification of *cyp11a2* exon 5 was carried out in 20µl reaction
148 with 1µl genomic DNA template, 1µl forward primer (10µM, 5'-
149 TTTAAGACCACCTCGCCCAT-3') and reverse primer (10µM, 5'-
150 GAGCCAGATTCAAACCAGCA-3') using FIREPol® Master Mix system (Solis
151 Biodyne, Tartu, Estonia). The PCR product was analyzed on a 2.5% (w/v)
152 agarose gel for any indel mutations.
153

154 **Analysis of visual background adaptation (VBA)**

155 To identify *cyp11a2*$^{-/-}$ mutants for defective VBA behavior, larvae were analyzed
156 at 96hpf as described previously (Griffin *et al.*, 2016). Briefly, larvae were
157 maintained in a dark environment for at least 60 minutes, followed by exposure

158 to bright illumination for 30 minutes. Larvae were then scored using a stringent
159 criterion for lack of melanophore contraction, as an indicator of defective VBA.
160 Only larvae with strongly dark pigmentation were designated as VBA-negative
161 (VBA-) while only the lightest ones were designated as VBA-positive (VBA+)
162 (Figure 1C). Larvae with ambiguous pigmentation level were discarded. The
163 groups of larvae with either dark or light pigmentation were then genotyped to
164 confirm the accuracy of VBA analysis.
165
166 **Steroid hormones measurements by LC-MS/MS**
167 Since over 90% VBA- larvae were confirmed to be *cyp11a2*$^{-/-}$ mutants
168 (Supplementary Table 2), we used this method to identify homozygous mutants
169 and wild-type siblings for steroid hormone measurements in larvae. Three
170 clutches of 150 VBA+ larvae and 150 VBA- larvae were collected at 120hpf into
171 a silanized tube and snap frozen on dry ice. 1ml of 1xPBS was added to the
172 samples, and the samples were lysed through four rounds of freeze-thawing.
173 After lysis the samples were homogenized with a pestle homogenizer and
174 freeze-dried. The whole bodies of adult wild-type siblings and *cyp11a2*$^{-/-}$
175 mutants at 180dpf (8 biological replicates each) were snap frozen on dry ice.
176 The adult samples were homogenized at 2,000rpm for 1 minute using a Mikro-
177 Dismembrator S (Sartorius, Gottingen, Germany) and then freeze-dried.
178 Approximately 100mg of the dried samples were transferred to a glass test tube
179 and resuspended in 900µl MilliQ water and 100µl MilliQ water containing
180 internal standard (15ng D4-cortisol, D7-11β-hydroxyandrostenedione, D7-
181 androstenedione and 1.5ng D2-testosterone). The steroids were extracted
182 twice using 3ml Methyl tert-butyl ether (MTBE). Following centrifugation for 5
183 minutes at low speed the MTBE fractions for each sample were pooled and
184 dried under a stream of nitrogen at 45°C. The dried residue was resuspended

185 in 150µl 50% (v/v) methanol prior to analysis. Steroids were separated and
186 quantified using an Acquity UPLC System (Waters, Milford, CT) coupled to a
187 Xevo TQ-S tandem mass spectrometer (Waters, Milford, CT) as previously
188 described (O'Reilly *et al.*, 2017).
189
190 **Induction of osmotic stress**
191 Three clutches of 25 VBA+ and VBA- larvae were collected at 120hpf. Larvae
192 were treated in 250mM sodium chloride (in E3 medium) for 20 minutes.
193 Subsequently, larvae were washed and incubated in E3 medium for 4 hours
194 before sampling for RNA extraction (Griffin *et al.*, 2016).
195
196 **Comparative gene expression analysis by quantitative Real-Time PCR**
197 **(qRT-PCR)**
198 Three clutches of 25 VBA+ and VBA- larvae were collected at 120hpf. Gonad,
199 pituitary and liver were collected from 3-5 male adult individuals. All the samples
200 were snap frozen on dry ice before processing. Total RNA from whole larvae
201 or adult tissues and reverse transcription were performed as previously
202 described (Griffin *et al.*, 2016). Oligonucleotide sequences are listed in
203 Supplementary Table 3. The qRT-PCR reaction was performed in 10µl volumes
204 on 384-well plates using PowerUP SYBR Green Master Mix (Applied
205 Biosystems, California, USA) on a 7900HT Fast Real-Time PCR System
206 (Applied Biosystems, California, USA). Expression levels for each gene were
207 normalized to reference gene *β-actin*, and fold changes were calculated relative
208 to wild-type siblings. Expression analysis of *pomca*, *fshb*, *lhb*, *fshr*, *lhcgr*, *gh1*
209 was performed using TaqMan Universal PCR Master Mix and TaqMan Gene
210 Expression Assays (Applied Biosystems, California, USA). Expression level
211 was then normalized to reference gene *ef1a.*

212

213 **Whole-mount RNA *in situ hybridization* (WISH)**

214 Whole-mount RNA *in situ hybridization* (WISH) was carried out following a
215 standard protocol (Thisse and Thisse, 2008). Briefly, 40 wild-type siblings and
216 40 *cyp11a2*$^{-/-}$ mutant larvae at 5dpf were fixed in 4% (w/v) paraformaldehyde
217 (PFA) in 1x PBS overnight and the next day were hybridized with *pomca* probe
218 at 70°C overnight. Larvae were then incubated with anti-digoxigenin-AP
219 antibody solution (1:4,000) overnight at 4°C and stained with NBT/BCIP until it
220 reached the desired intensity. The stained larvae were imaged using Leica
221 DFC420 camera (Leica Camera AG, Wetzlar, Germany). The *pomca* probe
222 was generated as previously described (Muthu *et al.*, 2016).

223

224 **Morphological analysis of adults**

225 The gross morphology of wild-type siblings and *cyp11a2*$^{-/-}$ mutants were
226 compared at 180dpf (n=10 for each genotype). The secondary sex
227 characteristics were examined based on a well-established method involving
228 body shape and coloration (Schilling, 2002, Dranow *et al.*, 2013). The
229 characterization was further confirmed by another two independent researchers
230 blinded to the genotype. The weight and length of adult zebrafish were
231 measured after being humanely euthanized. Subsequently, zebrafish were
232 dissected, gonads were examined and photographed.

233

234 **Breeding ability assessment and *in vitro* fertilization (IVF)**

235 A *cyp11a2*$^{-/-}$ mutant male or a wild-type sibling male was out-crossed to an
236 unrelated wild-type female in a breeding tank with a divider in the middle on the
237 afternoon prior to a breeding trial. The following morning, the divider separating
238 male and female fish was removed and they were allowed to mate. The number

239 of fertilized eggs was counted after 3 hours.

240 For IVF experiments, sperm were collected by dissecting the testes of
241 euthanized males, which were then homogenized in 50μl Hank's balanced salt
242 solution prepared as previously described (Kroeger *et al.*, 2014). Eggs were
243 collected from anesthetized wild-type females by gentle palpation of the
244 abdomen. 20μl of sperm solution was mixed with the clutch of collected eggs,
245 followed by 1ml of E3 medium to activate the sperm. After 2 minutes, further
246 E3 medium was added and eggs were incubated at 28.5°C for development
247 (Westerfield, 2000). Fertilization of eggs was confirmed by visualization under
248 a dissecting microscope.

249

250 **Mating behavior analysis**

251 A *cyp11a2*$^{-/-}$ mutant male or wild-type male sibling was paired with a wild-type
252 female in the late afternoon with a divider in the middle of the breeding tank.
253 The next morning, the divider was removed and breeding behaviors was
254 recorded from above the tank using the Zebralab software (Viewpoint Life
255 Sciences, Inc., Montreal, Canada). Videos of the breeding behaviors were then
256 analyzed. The frequency and duration of intimate contacts, including parallel
257 swimming, chasing and spawning, were recorded.

258

259 **Sperm counting**

260 Sperm were collected by dissecting the testes of euthanized males, followed
261 by homogenization in a 100x mass:volume dilution with 600 mOsm/kg Hank's
262 balanced salt solution prepared as described (Jing *et al.*, 2009). 10μl of sperm
263 solution was transferred to each counting chamber of a dual-chamber Improved
264 Neubauer hemocytometer (Hawksley, Sussex, UK) and sperm from each
265 sample were counted in duplicate according to the protocol specified in WHO

266 Laboratory manual for the examination and processing of human semen (World
267 Health Organization, 2010). A minimum of 200 sperms was counted for each
268 replicate. Sperm concentration was determined by calculating the
269 concentration per nanolitre and multiplying this by the weight to volume dilution
270 factor. The gonadosomatic index (GSI) was calculated using the formula
271 [gonad weight / total tissue weight] × 100.
272

273 **Hematoxylin and eosin (H&E) staining**

274 Adult fish were fixed in 4% (w/v) paraformaldehyde (PFA) in 1xPBS for 4 days
275 at 4°C followed by brief washing in 1xPBS. Fish were decalcified in 0.25M
276 EDTA pH8.0 for 4 days at room temperature and then transferred to 70% (v/v)
277 ethanol for storage at 4°C. The head, caudal fins and anal fins of the zebrafish
278 were removed and the samples were transferred to a tissue processor (Leica
279 TP2010) for dehydration and paraffin infiltration. After the pre-processing, the
280 samples were embedded in paraffin wax and 5μm sections were cut through
281 the entire gonad. For H&E staining samples were dewaxed using xylene and
282 rehydrated by transferring through a series of ethanol baths. Samples were
283 then stained with Gill's hematoxylin for 1 minute before dehydration in ethanol.
284 Samples were stained with 1% eosin in 95% (v/v) ethanol for 30 seconds and
285 subsequently washed in absolute ethanol for three times. Samples were
286 transferred to xylene and mounted using DPX mountant. The mounted samples
287 were left dry for overnight and imaged using Leica DFC420 camera (Leica
288 Camera AG, Wetzlar, Germany).
289

290 **Statistical analysis**

291 Statistical analysis and graphics were performed using Graphpad Prism 7.0c
292 (GraphPad Software, California, United States). For the comparison of means

293 between two samples, unpaired *t*-tests were used. For the comparison of
294 means of more than two samples, one- or two-way analysis of variance
295 (ANOVA) and Sidak's multiple comparisons test was used.

296 ## Results

297 **Generation of *cyp11a2* null alleles in zebrafish with CRISPR/Cas9**

298 To fully understand the function of *cyp11a2* in zebrafish larvae and adults, we
299 disrupted the *cyp11a2* gene employing a CRISPR/Cas9 strategy. gRNA was
300 designed to target a 18bp site (AATATCTACAGACAATTG) in exon 5 for
301 generation of a 5-prime disruption within the *cyp11a2* gene. Genomic disruption
302 in the germline of injected embryos was detected by conventional PCR. Sanger
303 sequencing of the F1 generation identified three different heritable alleles within
304 the targeted region. Two lines were subsequently maintained (*cyp11a2*^{SH565},
305 *cyp11a2*^{SH567}). The *cyp11a2*^{SH565} line has a 161bp deletion (c.818_978del)
306 spanning the entire exon 5, introducing a frameshift with a premature stop at
307 amino-acid position 282 (p.A273DfsX10) (Figure 1A-B). The second line
308 *cyp11a2*^{SH567} carried a 144bp deletion (c.821_964del), subsequently causing a
309 48 amino-acid in-frame deletion (p.274_321del) (Figure 1A-B). Thus, both
310 mutations are predicted to abolish Cyp11a2 activity.

311 The phenotypes of *cyp11a2* homozygous mutant larvae were characterized
312 before 5dpf. *cyp11a2*^{SH565} *and cyp11a2*^{SH567} homozygous mutants were
313 morphologically similar to control siblings during early development. The
314 c*yp11a2*^{SH565} line was used for subsequent analysis and will be named
315 *cyp11a2*$^{-/-}$ hereafter.

316 Background adaptation in zebrafish has been associated with impaired
317 glucocorticoid biosynthesis and signaling (Griffin *et al.*, 2016, Eachus *et al.*,
318 2017). Larvae from a heterozygous in-cross were analyzed by VBA
319 assessment at 96hpf and sorted into groups with either dark or light
320 pigmentation (Figure 1C). Subsequent genotyping revealed over 90% of VBA-
321 negative larvae were *cyp11a2*$^{-/-}$ mutants (Supplementary Table 2). VBA-
322 positive larvae were either wild-type or *cyp11a2*$^{+/-}$, confirming that *cyp11a2*$^{-/-}$

323 mutants are reliably identified by VBA assessment.

324

325 **Impaired steroid biosynthesis and systemic changes in *cyp11a2*$^{-/-}$ mutant**
326 **larvae**

327 To assess the importance of Cyp11a2 in steroidogenesis, we measured cortisol
328 concentrations by LC-MS/MS in *cyp11a2*$^{-/-}$ larvae. At 96hpf, larvae from a
329 heterozygous in-cross were sorted by VBA assessment into VBA+ and VBA-
330 groups (150 larvae in each group, 3 replicates). Steroid hormone profiles were
331 analyzed at 120hpf. The cortisol concentration was significantly reduced in
332 *cyp11a2*$^{-/-}$ mutants compared to their siblings (p=0.0143) (Figure 2A).
333 To further analyze the loss of Cyp11a2 on glucocorticoid action, qRT-PCR was
334 used to assay the transcriptional responses of glucocorticoid-inducible genes
335 after exposure to osmotic stress. Transcription of the glucocorticoid-responsive
336 genes *fkbp5* (p<0.0001) and *pck1* (p=0.0135) was significantly decreased in
337 *cyp11a2*$^{-/-}$ mutant larvae compared to siblings, when maintained under basal
338 conditions (Figure 2B-C). Exposure to osmotic stress resulted in a significant
339 increase in the expression of both *fkbp5* (p<0.0001) and *pck1* (p=0.0088) in
340 wild-types, but this treatment had no significant effect on expression levels of
341 these genes in *cyp11a2*$^{-/-}$ larvae (Figure 2B-C).
342 Moreover, impaired cortisol biosynthesis led to significantly higher levels of
343 *pomca* expression measured by qRT-PCR in *cyp11a2*$^{-/-}$ larvae (p=0.001)
344 (Figure 3A), suggesting activation of the HPI axis due to lack of negative
345 feedback. This finding was confirmed by WISH showing increased staining of
346 a *pomca* probe in pituitary tissue in *cyp11a2*$^{-/-}$ larvae compared with wild-type
347 siblings (Figure 3B).

348

349 **Cyp11a2-deficiency causes the development of only male fish with partly**

350 **feminized secondary sex characteristics**

351 Despite their profound glucocorticoid deficiency, *cyp11a2*$^{-/-}$ zebrafish develop
352 into viable adults. Typically, wild-type adult male zebrafish have a slender body
353 shape with pinkish-yellow coloration, whereas wild-type females have an egg-
354 filled abdomen of bluish-silver colour (Schilling, 2002, Dranow *et al.*, 2013). The
355 gross morphology of wild-type siblings and *cyp11a2*$^{-/-}$ mutants was compared
356 at 180dpf (n=10 for each genotype). All *cyp11a2*$^{-/-}$ animals had female-like
357 bluish-silver body pigmentation and an abdomen rounder than that of wild-type
358 males. Wild-type males had a dark yellow anal fin, compared to a light-yellow
359 colour of this structure in wild-type females. All *cyp11a2*$^{-/-}$ mutant animals had
360 a dark yellow-pigmented anal fin. However, similar to wild-type females,
361 *cyp11a2*$^{-/-}$ mutants displayed wider blue and narrower yellow stripes than wild-
362 type males (Figure 4A). Taken together, *cyp11a2*$^{-/-}$ mutants showed mixed
363 secondary sex characteristics with more pronounced female secondary sex
364 characteristics. Interestingly, the genital papilla was not apparent in all *cyp11a2*$^{-}$
365 $^{/-}$ fish, suggesting that their gonadal sex is male (Yossa *et al.*, 2013). Further
366 anatomical examination demonstrated that wild-type animals with male or
367 female secondary sex characteristics possessed testes or ovaries at similar
368 proportions (n=20). By contrast, all *cyp11a2*$^{-/-}$ mutants had testes and none had
369 ovaries (n=20) (Figure 4A). Interestingly, *cyp11a2*$^{-/-}$ mutant fish were found to
370 be significantly heavier (p=0.0132) and longer (p=0.001) than their wild-type
371 male and female siblings (Figure 4B-C). Further analysis on *gh1* (growth
372 hormone 1) showed significantly increased expression (p=0.001) in the testis
373 of *cyp11a2*$^{-/-}$ mutant adults (n=5) but no significant change in *gh1* expression
374 in the pituitary (p=0.1236) compared to wild-type siblings (n=5) (Figure 4D-E).

375

376 ***cyp11a2*$^{-/-}$ mutant adults are both glucocorticoid- and androgen-deficient**

377 To determine steroid hormone concentrations in adults, the whole bodies of
378 wild-type siblings and *cyp11a2*$^{-/-}$ mutants at 180dpf (8 biological replicates)
379 were used for LC/MS-MS analysis. Mutation of *cyp11a2* resulted in reduced
380 cortisol concentrations ($p<0.0001$) (Figure 5A). Systemic glucocorticoid
381 deficiency was confirmed by significantly decreased expression of *fkbp5*
382 ($p=0.0006$) and *pck1* ($p=0.0005$) in the livers of *cyp11a2*$^{-/-}$ adult animals,
383 compared to their siblings (Figure 5F-G). Furthermore, loss of *cyp11a2* function
384 caused significant reductions in the levels of androstenedione ($p<0.0001$), 11-
385 ketoandrostenedione ($p=0.0009$), testosterone ($p=0.0128$) and the active
386 zebrafish androgen, 11-ketotestosterone ($p=0.0038$) (Figure 5B-E).
387 Transcription of the known androgen-responsive gene *cyp2k22,* was also
388 markedly decreased in the livers of *cyp11a2*$^{-/-}$ males compared to their wild-
389 type siblings ($p=0.0003$) (Figure 5H).
390
391 **Cyp11a2-deficiency causes activation of the hypothalamic-pituitary-**
392 **gonadal axis (HPG axis)**
393 In response to the impaired sex steroid biosynthesis, significantly higher levels
394 of *fshb* ($p=0.0053$) and *lhb* ($p=0.0404$) transcripts were detected in the pituitary
395 of *cyp11a2*$^{-/-}$ mutant adults (n=5) compared to wild-type siblings (n=5)
396 (Supplementary Figure 1A-B), which may be caused by lack of negative
397 feedback due to androgen deficiency.
398
399 ***Cyp11a2*$^{-/-}$ homozygous adults are infertile**
400 Fertility of *cyp11a2*$^{-/-}$ fish was first assessed by out-crossing *cyp11a2*$^{-/-}$ mutants
401 or their wild-type male siblings with an unrelated wild-type female. In four
402 independent experiments, we found that wild-type males (n=10) could
403 successfully fertilize eggs produced by the females at a frequency of between

404 70-90%, whereas none of the pairs that included a *cyp11a2*$^{-/-}$ mutant (n=10)
405 could produce fertilized eggs (Supplementary Figure 2A). We also examined
406 the breeding behavior of wild-type male siblings (n=6) and *cyp11a2*$^{-/-}$ mutants
407 (n=6) out-crossed with unrelated wild-type females. Wild-type males exhibited
408 typical breeding behaviours, i.e. chasing wild-type females, making intimate
409 contacts and inducing spawning (Supplementary Figure 2B-C). However,
410 *cyp11a2*$^{-/-}$ mutants exhibited greatly reduced levels of chasing and intimate
411 contact with wild-type females (Supplementary Figure 2B-C). Consequently,
412 this resulted in failure of spawning induction in females.
413 Sperm concentration was then examined and found significantly decreased in
414 *cyp11a2*$^{-/-}$ mutants compared to wild-type siblings (p=0.0071) (Figure 6A).
415 Fertility of *cyp11a2*$^{-/-}$ mutants was further assessed by IVF. Interestingly, sperm
416 from the dissected testis (n=5) could not fertilize any wild-type eggs (p<0.0001),
417 compared to 50-90% fertilization rate by wild-type sperm (Figure 6B).
418 Taken together, our results suggested that loss of *cyp11a2* function
419 considerably impairs the fertility of adult males.
420
421 **Homozygous *cyp11a2*$^{-/-}$ mutant fish exhibit defective spermatogenesis**
422 **and disorganized testes**
423 The finding of a low sperm count and the absence of breeding behaviours in
424 *cyp11a2*$^{-/-}$ mutants led us to examine testicular structures and functions.
425 Histological analysis using H&E staining showed well-organized testes in wild-
426 type siblings. These testes had well-defined seminiferous tubules separated by
427 thin strands of interstitial connective tissue. Spermatozoa were located in the
428 center of each tubular lumen, with spermatids, spermatocytes and
429 spermatogonia located more peripherally, towards the basement membrane
430 (Figure 6C-D).

431 By contrast, the testes of *cyp11a2*$^{-/-}$ mutants were markedly disorganized and
432 adjacent seminiferous tubule cross-sections were difficult to distinguish from
433 one another. For each tubule cross-section, the central lumen was difficult to
434 identify, and mature spermatozoa were very rarely found within the testis.
435 Spermatogonia were the main cell type found in the testes of *cyp11a2*$^{-/-}$
436 mutants, with spermatocytes being the second dominant cell type (Figure 6E-
437 F). Interestingly, there was no difference in gonadosomatic index between
438 *cyp11a2*$^{-/-}$ mutant and wild-type siblings at 180dpf (Supplementary Figure 2D).
439

440 **Cyp11a2-deficiency causes downregulation of key genes involved in**
441 **testis development and spermatogenesis**

442 To investigate the molecular mechanisms underlying the phenotypic defects
443 observed, we used qRT-PCR to examine the transcription of genes involved in
444 testis development and spermatogenesis.
445 Doublesex and mab-3 related transcription factor 1 (*dmrt1*) is a key regulator of
446 testis development, and anti-Mullerian hormone (*amh*) is a pro-testis hormone
447 during zebrafish development. Interestingly, the expression of both genes was
448 decreased in the testes of *cyp11a2*$^{-/-}$ mutants (*dmrt1,* p=0.0151; *amh,*
449 p=0.0002) (Figure 7A-B). Furthermore, SRY-box 9a (*sox9a*), a pro-male
450 transcription factor involved in ovary-testis transition in zebrafish, is also
451 significantly downregulated (p=0.0249) (Figure 7C).
452 Insulin-like growth factor 3 (*igf3*) and insulin-like peptide 3 (*insl3*) are both
453 involved in the proliferation and differentiation of type A spermatogonia in the
454 early stages of spermatogenesis (Crespo *et al.*, 2016, Safian *et al.*, 2016).
455 Significant downregulation of *igf3* (p=0.001) (Figure 7D) and *insl3* (p=0.0006)
456 were found in *cyp11a2*$^{-/-}$ testes (Figure 7E), consistent with the findings of
457 decreased sperm quantity. The transcript level of inhibin alpha (*inha*) was

458 almost completely extinguished in testes from *cyp11a2*$^{-/-}$ mutants (p<0.0001)
459 (Figure 7F).
460 To further investigate molecular mechanisms of the decreased expression of
461 *igf3* and *insl3*, we examined the expression of *fshr* and *lhcgr* in the testes of
462 both mutant and wild-type sibling adults. However, no significant difference was
463 detected for either *fshr* (p=0.2481) or *lhcgr* (p=0.1372) (Supplementary Figure
464 1C-D).
465
466 **Differential expression of spermatogenesis markers in *cyp11a2***
467 **homozygous mutants**
468 To investigate how loss of *cyp11a2* function impacts on spermatogenesis, we
469 measured the expression of germ cell markers at several stages of
470 spermatogenesis. *nanos2* is expressed in type A undifferentiated
471 spermatogonia while *piwil1* is expressed in all type A spermatogonia (Beer and
472 Draper, 2013, Safian *et al.*, 2016). We found a significant upregulation of
473 *nanos2* (p=0.0004) and *piwil1* (p=0.022) expression in the testes of *cyp11a2*$^{-/-}$
474 fish. No change was found in the expression of *dazl*, a marker of type B
475 spermatogonia (p=0.8219) (Safian *et al.*, 2016). Interestingly, expression of
476 spermatocyte marker *sycp3* (p=0.0012) and spermatid marker *odf3b*
477 (p=0.0003) was significantly downregulated (Figure 8A-E) (Ozaki *et al.*, 2011,
478 Tang *et al.*, 2018). The expression profile is consistent with the assessment of
479 sperm quality and quantity, suggesting decreased numbers of late stage germ
480 cells and accumulation of germ cell precursors.

481 ## Discussion

482 Previous data by our group and others (Hsu *et al.*, 2009, Parajes *et al.*, 2013)
483 suggested that *cyp11a1* is expressed during early development stages from
484 zygote to 24hpf, while the expression of *cyp11a2* becomes continuously
485 prominent just before *de novo* (48hpf) and HPI-mediated (96hpf) cortisol
486 synthesis commences (Weger *et al.*, 2018, Parajes *et al.*, 2013). Further *in situ*
487 *hybridization* analysis showed the expression of *cyp11a2* is restricted to the
488 interrenal at 120hpf, whereas no expression of *cyp11a1* was found (Weger *et*
489 *al.*, 2018). Functional analysis using transient morpholino knockdown in larvae
490 revealed distinct roles between the two genes. *cyp11a1* is required for early
491 embryonic development, which is consistent with observations in other reports
492 (Goldstone *et al.*, 2010). *cyp11a2* is essential for *de novo* steroidogenesis in
493 zebrafish larvae and appeared to be the functional equivalent of human
494 *CYP11A1* (Parajes *et al.*, 2013). In this study, we confirmed previously reported
495 results and clarified the role of Cyp11a2 in adult zebrafish using stable null-
496 allele lines.

497

498 **Disruption of *cyp11a2* leads to glucocorticoid deficiency**

499 Previous morpholino knockdown of *cyp11a2* showed various levels of
500 phenotypic abnormalities including craniofacial defects, pericardiac oedema
501 and absence of swim bladder (Parajes *et al.*, 2013). Similar phenotypes were
502 found in loss of *ff1b* (ortholog of mammalian steroidogenic factor 1) or *dax1*,
503 but all the studies were based on morpholinos (Chai *et al.*, 2003, Zhao *et al.*,
504 2006). In contrast, these phenotypes were absent in our newly generated
505 *cyp11a2*$^{-/-}$ knockout lines and such phenotypes have also not been observed
506 in our published glucocorticoid-deficient lines due to 21-hydroxylase (Eachus
507 *et al.*, 2017) or ferredoxin deficiency (Griffin *et al.*, 2016). Morpholinos are well

508 known for their off-target effects (Eisen and Smith, 2008) and thus the
509 previously described changes attributed to glucocorticoid deficiency (Parajes *et*
510 *al.*, 2013) are more likely caused by morpholino toxicity (Stainier *et al.*, 2017).
511 Our *cyp11a2*$^{-/-}$ mutants displayed typical characteristics of glucocorticoid
512 deficiency. VBA is a glucocorticoid-dependent neuroendocrine response
513 mediated via the Glucocorticoid Receptor (Muto *et al.*, 2005, Muto *et al.*, 2013).
514 Impaired VBA has been previously described in several zebrafish lines with
515 defective glucocorticoid signaling (Eachus *et al.*, 2017, Griffin *et al.*, 2016,
516 Facchinello *et al.*, 2017). The VBA analysis of larvae at 120hpf revealed that
517 about 93% of the strongly dark pigmented larvae were *cyp11a2*$^{-/-}$ mutants,
518 suggesting impaired glucocorticoid biosynthesis.
519 Adrenal insufficiency causes an upregulation of the hypothalamus-pituitary-
520 adrenal axis in humans due to a disruption of the negative HPA feedback
521 (Liyanarachchi *et al.*, 2017). Our *cyp11a2*$^{-/-}$ mutants exhibited an upregulation
522 of the HPI axis as indicated by increased *pomca* expression (Figure 3). This is
523 consistent with other zebrafish models of glucocorticoid resistance (Ziv *et al.*,
524 2013, Lin *et al.*, 2015) and glucocorticoid deficiency (Griffin *et al.*, 2016, Eachus
525 *et al.*, 2017) due to loss of negative feedback to the pituitary and hypothalamus.
526 The significantly decreased concentration of cortisol in the VBA- larvae clearly
527 demonstrates the requirement for Cyp11a2 to enable glucocorticoid
528 biosynthesis, which is consistent with our previous morpholino knockdown
529 study (Parajes *et al.*, 2013). However, some baseline cortisol production was
530 detected in VBA- larvae. The most plausible explanation is that a small
531 proportion of wild-type or heterozygous siblings are also VBA- but designated
532 as *cyp11a2*$^{-/-}$ mutant larvae. This limitation to the use of VBA as a genotyping
533 proxy has been highlighted previously (Eachus *et al.*, 2017). However, the lack
534 of detectable concentrations of cortisol in *cyp11a2*$^{-/-}$ adults confirmed that they

535 are glucocorticoid deficient. To further validate this model of glucocorticoid
536 deficiency, we subjected the larvae to osmotic stress, which has previously
537 been used to induce cortisol production (Weger *et al.*, 2012). However, there
538 was no transcriptional increase of either *fkbp5* or *pck1* in the *cyp11a2*$^{-/-}$ mutant
539 larvae under osmotic stress, further demonstrating a block in glucocorticoid
540 biosynthesis.
541
542 **Disruption of *cyp11a2* leads to sex steroid deficiency and all-male fish**
543 **with feminized secondary sex characteristics (SSCs)**
544 Sex steroids are required for sexual development and are also responsible for
545 the maintenance of established sex phenotypes (Goppert *et al.*, 2016). We
546 found significantly reduced concentrations of the sex steroid precursor
547 androstenedione, the active zebrafish androgen 11-ketotestosterone, and
548 testosterone in *cyp11a2*$^{-/-}$ adult mutants. All *cyp11a2*$^{-/-}$ mutant zebrafish
549 developed testes. Previous studies on *cyp19a1a* and *cyp17a1* in zebrafish
550 have shown all-male phenotypes (Zhai *et al.*, 2018, Lau *et al.*, 2016). Therefore,
551 our results suggest that the impaired biosynthesis of sex steroids in *cyp11a2*$^{-/-}$
552 mutant zebrafish is responsible for their all-male phenotype.
553 Cyp11a2-deficient male zebrafish mainly exhibited feminized SSCs, including
554 female body pigmentation and a rounded body shape. In teleost fish,
555 androgens, especially 11-ketotestosterone, are important for testicular
556 development and for the development of SSCs (Borg, 1994). Both testosterone
557 and 11-ketotestosterone have high affinity and transactivation potency for the
558 androgen receptor (Ar) in zebrafish (de Waal *et al.*, 2008, Hossain *et al.*, 2008).
559 Similarly, Ar-deficient zebrafish males also exhibited female-type coloration and
560 body shape (Crowder *et al.*, 2018, Yu *et al.*, 2018). Moreover, feminized SSCs
561 were also demonstrated in the Cyp17a1-deficient zebrafish males; however,

562 this androgen-deficient line exhibited a slender body shape as found in wild-
563 type males (Zhai *et al.*, 2018). Taken together, these results suggest that the
564 development of male SSCs requires appropriate androgen exposure. However,
565 the cause of observed phenotypic variability in different androgen-deficient
566 lines remains to be elucidated.
567
568 ***cyp11a2*$^{-/-}$ mutants exhibit male infertility**
569 Our *cyp11a2*$^{-/-}$ mutants failed to exhibit male-typical chasing activity and the
570 ability to induce female spawning during natural breeding. Similarly, Ar-deficient
571 zebrafish and androgen-deficient *cyp17a1* knockout zebrafish exhibit defective
572 breeding behaviours (Zhai *et al.*, 2018, Crowder *et al.*, 2018, Tang *et al.*, 2018,
573 Yu *et al.*, 2018). Ar is necessary for zebrafish fertility, and male mating
574 behaviors are likely to be regulated by androgen signaling. Further fertility
575 assessment by sperm counting revealed significantly reduced sperm
576 concentrations in *cyp11a2*$^{-/-}$ mutants, indicating impaired spermatogenesis. A
577 lower amount of mature spermatozoa was also observed in the testes of
578 zebrafish *ar*$^{-/-}$ mutants (Crowder *et al.*, 2018, Tang *et al.*, 2018, Yu *et al.*, 2018).
579 Interestingly, normal spermatogenesis was found in Cyp17a1-deficient
580 zebrafish mutants, possibly due to compensation by Cyp17a2 (Zhai *et al.*,
581 2018). However, biochemical analysis suggested zebrafish Cyp17a2 cannot
582 catalyze the 17,20-lyase reactions that yield to DHEA and androstenedione
583 (Pallan *et al.*, 2015). Progesterone has been suggested to function in
584 spermatogonial cell proliferation and spermatogenesis in teleosts (Liu *et al.*,
585 2014, Wang *et al.*, 2016). Moreover, the specificity of the interactions between
586 Ar and its ligands are not fully characterized in teleosts. The development of
587 relatively normal testes with mature spermatozoa in *cyp17a1* mutant animals
588 might be explained by some affinity of Ar for progesterone (de Waal *et al.*,

589 2008).

590 In mammals, androgen signaling is believed to be required for testis
591 development and spermatogenesis. A murine *Cyp11a1* deletion model had
592 testes with disorganized seminiferous tubules containing only spermatocytes
593 arrested at the meiotic stage (Hu *et al.*, 2002). Our histological analysis of the
594 testes from *cyp11a2*$^{-/-}$ mutants showed poorly defined seminiferous tubules
595 without a distinguishable central lumen. Moreover, the seminiferous tubules
596 mainly contained spermatogonia and very few spermatocytes or mature
597 spermatozoa. Similarly, zebrafish *ar*$^{-/-}$ mutants also exhibit disorganized
598 seminiferous tubules replete with spermatogonia and spermatocytes but
599 deficient in mature spermatozoa (Yu *et al.*, 2018, Crowder *et al.*, 2018).

600 Whilst the molecular mechanism underlying the severe disruption of
601 spermatogenesis in Cyp11a2-deficient zebrafish remains elusive, our
602 observations of markedly reduced *igf3* and *insl3* expression may contribute to
603 the accumulation of early spermatogonial cells as Igf3 and Insl3 are both
604 involved in the proliferation and differentiation of type A spermatogonia (Crespo
605 *et al.*, 2016, Safian *et al.*, 2016, Assis *et al.*, 2016). Downregulation of *igf3* and
606 *insl3* was previously reported in *ar*-null mutants (Tang *et al.*, 2018). Moreover,
607 unchanged level of *dazl* expression, a marker of type B spermatogonia,
608 suggests normal differentiation from type A to type B spermatogonia. On the
609 other hand, the reduced expression of the spermatocyte marker *sycp3* and
610 spermatid marker *odf3b* indicate that the transition into and/or completion of
611 meiosis are compromised.

612

613 In this study, we generated *cyp11a2* knockout animals by employing
614 CRISPR/Cas9 gene editing technology. These *cyp11a2*-null mutant zebrafish
615 are deficient in both glucocorticoid and sex steroids. We demonstrated the

phenotypic consequences of the combined steroid hormone deficiencies. This work thus establishes a requirement for Cyp11a2 in adrenal and gonadal steroidogenesis in zebrafish.

Declaration of interest

The authors declare that there is no conflict of interest that could be perceived as prejudicing the impartiality of the research reported.

Funding

This work was supported by the International Fund Congenital Adrenal Hyperplasia 2017 research grant (awarded to N.K. and V.T.C) and the Deutsche Forschungsgemeinschaft (KR 3363/3-1).

Acknowledgements

The authors would like to thank all the aquarium staff in the University of Sheffield for maintenance of fish stocks, Maggie Glover for help with histological analysis.

633 **Figure legends**

634 **Figure 1. Generation of *cyp11a2* null-allele using CRIPSR/Cas9 strategy.**
635 A) Exon 5 of cyp11a2 was targeted for genetic disruption by CRISPR/Cas9.
636 *Cyp11a2*^{SH565} has a 161bp deletion with the whole exon 5 deleted, resulting in
637 a truncated protein of 282aa. *Cyp11a2*^{SH567} has a deletion of 144bp leading to
638 a truncated protein of 464aa. B) Gel electrophoresis shows genotyping of wild-
639 type, heterozygotes and homozygotes by PCR. C) *cyp11a2*$^{-/-}$ mutant larvae
640 (120dpf) had impaired visual-mediated background adaption. Scale bar:
641 300μm.

642 **Figure 2. Zebrafish *cyp11a2*$^{-/-}$ mutant larvae are glucocorticoid deficient.**
643 A) LC-MS/MS showed significantly reduced level of cortisol in *cyp11a2*
644 homozygous mutant larvae at 120hpf (unpaired *t* test). Analysis of baseline and
645 stress-induced transcript levels of A) *fkbp5* and B) *pck1* using qRT-PCR in
646 120hpf siblings and homozygous larvae (two-way ANOVA). *, $p<0.05$; **,
647 $p<0.005$; ***, $p<0.0005$; ****, $p<0.0001$.

648 **Figure 3. Zebrafish *cyp11a2*$^{-/-}$ mutants have a dysregulated HPI axis at**
649 **120hpf.** A) qRT-PCR analysis of the expression of *pomca* was significantly
650 upregulated in *cyp11a2*$^{-/-}$ mutant larvae (unpaired *t* test, ***$p=0.001$). B) WISH
651 analysis showed the expression of *pomca* was increased in *cyp11a2*$^{-/-}$ mutant
652 larvae compared to wild-type. Scale bar: 0.3mm.

653 **Figure 4. Depletion of Cyp11a2 leads to all-male homozygous fish.** A)
654 Cyp11a2-deficiency caused fish to develop only into males as seen with the
655 presence of testes and an apparent absence of the genital papilla. The
656 *cyp11a2*$^{-/-}$ fish mainly exhibited feminized secondary sex characteristics. Scale
657 bar: 1mm. Adult *cyp11a2*$^{-/-}$ zebrafish exhibited increased B) weight and C)
658 length compared to wild-type siblings. D) Expression of *gh1* was significantly
659 increased in the testes of *cyp11a2*$^{-/-}$ mutant adults compared to that of wild-type

660 adult males (n=5). E) Expression of *gh1* was unchanged in the pituitary of
661 *cyp11a2*$^{-/-}$ mutant adults compared to wild-type adult males (n=5). An unpaired
662 *t* test was used for the analysis. *, p<0.05; **, p<0.005.

663 **Figure 5. Zebrafish *cyp11a2*$^{-/-}$ mutant adults have impaired interrenal and**
664 **gonadal steroid hormone biosynthesis.** The concentration of A) cortisol, sex
665 steroids and their precursors B) androstenedione, C) 11-ketoandrostenedione,
666 D) testosterone, and E) 11-ketotestosterone were significantly decreased in
667 *cyp11a2*$^{-/-}$ adult males compared to wild-type siblings (n=8). Transcript levels
668 of F) *fkbp5* and G) *pck1* were also significantly decreased in *cyp11a2*$^{-/-}$ adult
669 liver compared to the livers of wild-type siblings (n=5). H) Expression of the
670 androgen-responsive gene *cyp2k22* was almost completely extinguished in the
671 liver of *cyp11a2*$^{-/-}$ adult males (n=5). An unpaired *t* test was used for all analysis.
672 *, p<0.05; **, p<0.005; ***, p<0.0005.

673 **Figure 6. *Cyp11a2*$^{-/-}$ homozygous male adults are infertile.** A) Sperm
674 concentration was markedly reduced in *cyp11a2*$^{-/-}$ mutant males (n=4). B)
675 Sperm from the dissected testis of the *cyp11a2*$^{-/-}$ mutants (n=5) could not
676 fertilize any wild-type eggs, compared to 50-90% fertilization rate by wild-type
677 sperm. C-F) Histological analysis of testes at 180dpf showed that *cyp11a2*$^{-/-}$
678 mutants (E-F) had disorganized seminiferous tubules with a barely
679 distinguishable central lumen compared to the testes of wild-type males (C-D).
680 Spermatogonia were the main cell type found in the mutant testes, with some
681 spermatocytes and a very few spermatozoa also present. SG, spermatogonia;
682 SC, spermatocyte; SZ, spermatozoa. Scale bar: 10 μm. An unpaired *t* test was
683 used for the analysis. **, p<0.005, ****, p<0.0001.

684 **Figure 7. Expression of pro-testis and spermatogenic genes was**
685 **downregulated in the testes of *cyp11a2*$^{-/-}$ zebrafish.** A-F) Relative
686 expression of *dmrt1*, *amh*, *sox9a, igf3*, *insl3* and *inha* were significantly

687 decreased in the testes of homozygous mutants compared to wild-type siblings
688 (n=5). An unpaired *t* test was used for all analysis. *, p<0.05; **, p<0.005; ***,
689 p<0.0005, ****, p<0.0001.

690 **Figure 8. Spermatogenesis markers were differentially expressed in the**
691 **testes of *cyp11a2*$^{-/-}$ mutant and wild-type adults.** Expression of A) *nanos2*
692 and B) *piwil1*, which are markers for type A_{und} spermatogonia and all type A
693 spermatogonia, respectively, was significantly increased in the testes of
694 homozygous mutants (n=5). C) Expression of *dazl*, a marker of type B
695 spermatogonia, was not changed (n=5). Expression of the spermatocyte
696 marker D) *sycp3,* and the spermatid marker, E) *odf3b* was significantly
697 downregulated (n=5). An unpaired *t* test was used for all analysis. *, p<0.05; **,
698 p<0.005; ***, p<0.0005.

699 **Supplementary Fig 1. Expression levels of gonadotropin genes and their**
700 **receptors.** The transcript levels of A) *fshb* and B) *lhb* were significantly
701 upregulated in the pituitary of the *cyp11a2*$^{-/-}$ mutant adults (n=5). However, no
702 significant changes in the expression of C) *fshr* and D) *lhcgr* were found in the
703 testes of the *cyp11a2*$^{-/-}$ mutant adults (n=5). An unpaired *t* test was used for all
704 analysis. *, p<0.05; **, p<0.005.

705 **Supplementary Fig 2. Natural breeding behaviors are absent in *cyp11a2*$^{-/-}$**
706 **mutant zebrafish.** A) *cyp11a2*$^{-/-}$ male adults lacked natural breeding ability to
707 produce fertilised eggs when paired with wild-type females (n=10). B-C)
708 *cyp11a2*$^{-/-}$ male adults showed impaired natural mating behavior with
709 significantly reduced frequency and duration of intimate contacts compared to
710 wild-type males in a 5-minute period (n=6). D) There was no difference in
711 gonadosomatic index (GSI) between *cyp11a2*$^{-/-}$ mutant males and wild-type
712 siblings (n=5). An unpaired *t* test was used for all analysis. ***, p<0.0005; ****,
713 p<0.0001.

714 **Reference**

715 Assis LH, Crespo D, Morais RD, Franca LR, Bogerd J & Schulz RW 2016 INSL3
716 stimulates spermatogonial differentiation in testis of adult zebrafish (Danio rerio).
717 *Cell Tissue Res* **363** 579-88.
718 Beer RL & Draper BW 2013 nanos3 maintains germline stem cells and expression
719 of the conserved germline stem cell gene nanos2 in the zebrafish ovary. *Dev Biol*
720 **374** 308-18.
721 Borg B 1994 Androgens in teleost fishes. *Comparative Biochemistry and Physiology*
722 *Part C: Pharmacology, Toxicology and Endocrinology* **109** 219-245.
723 Chai C, Liu YW & Chan WK 2003 Ff1b is required for the development of
724 steroidogenic component of the zebrafish interrenal organ. *Dev Biol* **260** 226-44.
725 Crespo D, Assis LHC, Furmanek T, Bogerd J & Schulz RW 2016 Expression profiling
726 identifies Sertoli and Leydig cell genes as Fsh targets in adult zebrafish testis. *Mol*
727 *Cell Endocrinol* **437** 237-251.
728 Crowder CM, Lassiter CS & Gorelick DA 2018 Nuclear Androgen Receptor
729 Regulates Testes Organization and Oocyte Maturation in Zebrafish. *Endocrinology*
730 **159** 980-993.
731 de Waal PP, Wang DS, Nijenhuis WA, Schulz RW & Bogerd J 2008 Functional
732 characterization and expression analysis of the androgen receptor in zebrafish
733 (Danio rerio) testis. *Reproduction* **136** 225-34.
734 Dickmeis T 2009 Glucocorticoids and the circadian clock. *J Endocrinol* **200** 3-22.
735 Dranow DB, Tucker RP & Draper BW 2013 Germ cells are required to maintain a
736 stable sexual phenotype in adult zebrafish. *Dev Biol* **376** 43-50.
737 Eachus H, Zaucker A, Oakes JA, Griffin A, Weger M, Guran T, Taylor A, Harris A,
738 Greenfield A, Quanson JL, et al. 2017 Genetic Disruption of 21-Hydroxylase in
739 Zebrafish Causes Interrenal Hyperplasia. *Endocrinology* **158** 4165-4173.
740 Eisen JS & Smith JC 2008 Controlling morpholino experiments: don't stop making
741 antisense. *Development* **135** 1735-43.
742 Facchinello N, Skobo T, Meneghetti G, Colletti E, Dinarello A, Tiso N, Costa R,
743 Gioacchini G, Carnevali O, Argenton F, et al. 2017 nr3c1 null mutant zebrafish are
744 viable and reveal DNA-binding-independent activities of the glucocorticoid
745 receptor. *Sci Rep* **7** 4371.
746 Goldstone JV, McArthur AG, Kubota A, Zanette J, Parente T, Jonsson ME, Nelson DR
747 & Stegeman JJ 2010 Identification and developmental expression of the full
748 complement of Cytochrome P450 genes in Zebrafish. *BMC Genomics* **11** 643.
749 Goppert C, Harris RM, Theis A, Boila A, Hohl S, Ruegg A, Hofmann HA, Salzburger
750 W & Bohne A 2016 Inhibition of Aromatase Induces Partial Sex Change in a Cichlid
751 Fish: Distinct Functions for Sex Steroids in Brains and Gonads. *Sex Dev* **10** 97-110.
752 Griffin A, Parajes S, Weger M, Zaucker A, Taylor AE, O'Neil DM, Muller F & Krone N
753 2016 Ferredoxin 1b (Fdx1b) Is the Essential Mitochondrial Redox Partner for
754 Cortisol Biosynthesis in Zebrafish. *Endocrinology* **157** 1122-34.
755 Hossain MS, Larsson A, Scherbak N, Olsson PE & Orban L 2008 Zebrafish androgen
756 receptor: isolation, molecular, and biochemical characterization. *Biol Reprod* **78**
757 361-9.
758 Hruscha A, Krawitz P, Rechenberg A, Heinrich V, Hecht J, Haass C & Schmid B 2013
759 Efficient CRISPR/Cas9 genome editing with low off-target effects in zebrafish.
760 *Development* **140** 4982-7.
761 Hsu HJ, Lin JC & Chung BC 2009 Zebrafish cyp11a1 and hsd3b genes: structure,
762 expression and steroidogenic development during embryogenesis. *Mol Cell*
763 *Endocrinol* **312** 31-4.

764 Hu MC, Hsu NC, El Hadj NB, Pai CI, Chu HP, Wang CK & Chung BC 2002 Steroid
765 deficiency syndromes in mice with targeted disruption of Cyp11a1. *Mol Endocrinol*
766 **16** 1943-50.
767 Jing R, Huang C, Bai C, Tanguay R & Dong Q 2009 Optimization of activation,
768 collection, dilution, and storage methods for zebrafish sperm. *Aquaculture* **290**
769 165-171.
770 Kroeger PT, Jr., Poureetezadi SJ, McKee R, Jou J, Miceli R & Wingert RA 2014
771 Production of haploid zebrafish embryos by in vitro fertilization. *J Vis Exp*.
772 Lau ES, Zhang Z, Qin M & Ge W 2016 Knockout of Zebrafish Ovarian Aromatase
773 Gene (cyp19a1a) by TALEN and CRISPR/Cas9 Leads to All-male Offspring Due to
774 Failed Ovarian Differentiation. *Sci Rep* **6** 37357.
775 Lin JC, Hu S, Ho PH, Hsu HJ, Postlethwait JH & Chung BC 2015 Two Zebrafish hsd3b
776 Genes Are Distinct in Function, Expression, and Evolution. *Endocrinology* **156**
777 2854-62.
778 Liu G, Luo F, Song Q, Wu L, Qiu Y, Shi H, Wang D & Zhou L 2014 Blocking of
779 progestin action disrupts spermatogenesis in Nile tilapia (Oreochromis niloticus).
780 *J Mol Endocrinol* **53** 57-70.
781 Liu YW 2007 Interrenal organogenesis in the zebrafish model. *Organogenesis* **3**
782 44-8.
783 Liyanarachchi K, Ross R & Debono M 2017 Human studies on hypothalamo-
784 pituitary-adrenal (HPA) axis. *Best Pract Res Clin Endocrinol Metab* **31** 459-473.
785 Lohr H & Hammerschmidt M 2011 Zebrafish in endocrine systems: recent
786 advances and implications for human disease. *Annu Rev Physiol* **73** 183-211.
787 Miller WL & Auchus RJ 2011 The molecular biology, biochemistry, and physiology
788 of human steroidogenesis and its disorders. *Endocr Rev* **32** 81-151.
789 Muthu V, Eachus H, Ellis P, Brown S & Placzek M 2016 Rx3 and Shh direct
790 anisotropic growth and specification in the zebrafish tuberal/anterior
791 hypothalamus. *Development* **143** 2651-63.
792 Muto A, Orger MB, Wehman AM, Smear MC, Kay JN, Page-McCaw PS, Gahtan E, Xiao
793 T, Nevin LM, Gosse NJ, et al. 2005 Forward genetic analysis of visual behavior in
794 zebrafish. *PLoS Genet* **1** e66.
795 Muto A, Taylor MR, Suzawa M, Korenbrot JI & Baier H 2013 Glucocorticoid
796 receptor activity regulates light adaptation in the zebrafish retina. *Front Neural*
797 *Circuits* **7** 145.
798 O'Reilly MW, Kempegowda P, Jenkinson C, Taylor AE, Quanson JL, Storbeck KH &
799 Arlt W 2017 11-Oxygenated C19 Steroids Are the Predominant Androgens in
800 Polycystic Ovary Syndrome. *J Clin Endocrinol Metab* **102** 840-848.
801 Ozaki Y, Saito K, Shinya M, Kawasaki T & Sakai N 2011 Evaluation of Sycp3, Plzf
802 and Cyclin B3 expression and suitability as spermatogonia and spermatocyte
803 markers in zebrafish. *Gene Expr Patterns* **11** 309-15.
804 Pallan PS, Nagy LD, Lei L, Gonzalez E, Kramlinger VM, Azumaya CM, Wawrzak Z,
805 Waterman MR, Guengerich FP & Egli M 2015 Structural and kinetic basis of steroid
806 17alpha,20-lyase activity in teleost fish cytochrome P450 17A1 and its absence in
807 cytochrome P450 17A2. *J Biol Chem* **290** 3248-68.
808 Parajes S, Griffin A, Taylor AE, Rose IT, Miguel-Escalada I, Hadzhiev Y, Arlt W,
809 Shackleton C, Muller F & Krone N 2013 Redefining the initiation and maintenance
810 of zebrafish interrenal steroidogenesis by characterizing the key enzyme cyp11a2.
811 *Endocrinology* **154** 2702-11.
812 Safian D, Morais RD, Bogerd J & Schulz RW 2016 Igf Binding Proteins Protect
813 Undifferentiated Spermatogonia in the Zebrafish Testis Against Excessive
814 Differentiation. *Endocrinology* **157** 4423-4433.

815 Schilling TF 2002. The morphology of larval and adult zebrafish. *In:* NÜSSLEIN -
816 VOLHARD, C. D., RALF (ed.) *Zebrafish.* 1 ed. Oxford: Oxford University Press.
817 Stainier DYR, Raz E, Lawson ND, Ekker SC, Burdine RD, Eisen JS, Ingham PW,
818 Schulte-Merker S, Yelon D, Weinstein BM, et al. 2017 Guidelines for morpholino
819 use in zebrafish. *PLoS Genet* **13** e1007000.
820 Talbot JC & Amacher SL 2014 A streamlined CRISPR pipeline to reliably generate
821 zebrafish frameshifting alleles. *Zebrafish* **11** 583-5.
822 Tang H, Chen Y, Wang L, Yin Y, Li G, Guo Y, Liu Y, Lin H, Cheng CHK & Liu X 2018
823 Fertility impairment with defective spermatogenesis and steroidogenesis in male
824 zebrafish lacking androgen receptor. *Biol Reprod* **98** 227-238.
825 Thisse C & Thisse B 2008 High-resolution in situ hybridization to whole-mount
826 zebrafish embryos. *Nat Protoc* **3** 59-69.
827 To TT, Hahner S, Nica G, Rohr KB, Hammerschmidt M, Winkler C & Allolio B 2007
828 Pituitary-interrenal interaction in zebrafish interrenal organ development. *Mol*
829 *Endocrinol* **21** 472-85.
830 Tokarz J, Moller G, de Angelis MH & Adamski J 2013 Zebrafish and steroids: what
831 do we know and what do we need to know? *J Steroid Biochem Mol Biol* **137** 165-
832 73.
833 Tokarz J, Moller G, Hrabe de Angelis M & Adamski J 2015 Steroids in teleost fishes:
834 A functional point of view. *Steroids* **103** 123-44.
835 Wang C, Liu D, Chen W, Ge W, Hong W, Zhu Y & Chen SX 2016 Progestin increases
836 the expression of gonadotropins in pituitaries of male zebrafish. *J Endocrinol* **230**
837 143-56.
838 Weger BD, Weger M, Nusser M, Brenner-Weiss G & Dickmeis T 2012 A chemical
839 screening system for glucocorticoid stress hormone signaling in an intact
840 vertebrate. *ACS Chem Biol* **7** 1178-83.
841 Weger M, Diotel N, Weger BD, Beil T, Zaucker A, Eachus HL, Oakes JA, do Rego JL,
842 Storbeck KH, Gut P, et al. 2018 Expression and activity profiling of the
843 steroidogenic enzymes of glucocorticoid biosynthesis and the fdx1 co-factors in
844 zebrafish. *J Neuroendocrinol* **30** e12586.
845 Westerfield M 2000. The zebrafish book. A guide for the laboratory use of
846 zebrafish (Danio rerio). 4th ed. Eugene: Univ. of Oregon Press, .
847 World Health Organization DoRHaR 2010. WHO
848 Laboratory manual for the examination and processing of human semen. 5 ed.
849 Yossa R, Sarker PK, Proulx E, Saxena V, Ekker M & Vandenberg GW 2013 A
850 Practical Approach for Sexing Zebrafish,Danio rerio. *Journal of Applied*
851 *Aquaculture* **25** 148-153.
852 Yu G, Zhang D, Liu W, Wang J, Liu X, Zhou C, Gui J & Xiao W 2018 Zebrafish
853 androgen receptor is required for spermatogenesis and maintenance of ovarian
854 function. *Oncotarget* **9** 24320-24334.
855 Zhai G, Shu T, Xia Y, Lu Y, Shang G, Jin X, He J, Nie P & Yin Z 2018 Characterization
856 of Sexual Trait Development in cyp17a1-Deficient Zebrafish. *Endocrinology* **159**
857 3549-3562.
858 Zhao Y, Yang Z, Phelan JK, Wheeler DA, Lin S & McCabe ER 2006 Zebrafish dax1 is
859 required for development of the interrenal organ, the adrenal cortex equivalent.
860 *Mol Endocrinol* **20** 2630-40.
861 Ziv L, Muto A, Schoonheim PJ, Meijsing SH, Strasser D, Ingraham HA, Schaaf MJ,
862 Yamamoto KR & Baier H 2013 An affective disorder in zebrafish with mutation of
863 the glucocorticoid receptor. *Mol Psychiatry* **18** 681-91.
864

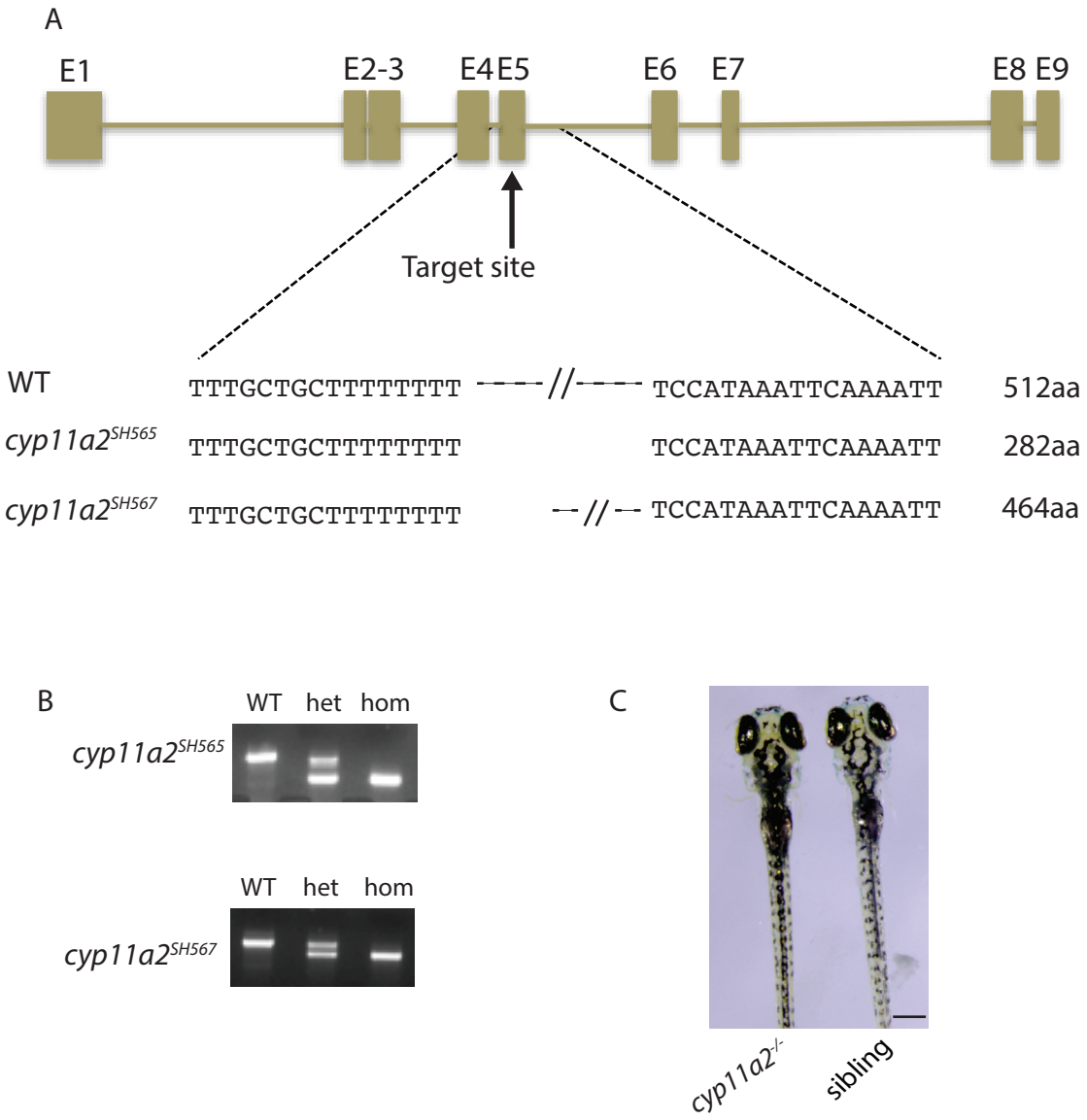
A
E1
E2-3
E4
E5
E6
E7
E8
E9
Target site
WT
TTTGCTGCTTTTTTTT
TCCATAAATTCAAAATT
512aa
cyp11a2SH565
TTTGCTGCTTTTTTTT
TCCATAAATTCAAAATT
282aa
cyp11a2SH567
TTTGCTGCTTTTTTTT
TCCATAAATTCAAAATT
464aa
B
WT
het
hom
cyp11a2SH565
WT
het
hom
cyp11a2SH567
C
cyp11a2-/-
sibling

A

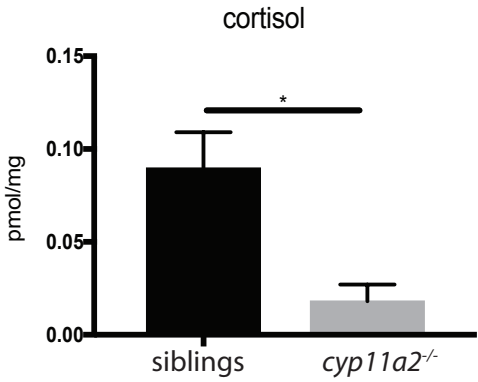
cortisol
0.15
0.10
0.05
0.00
pmol/mg
*
siblings
cyp11a2-/-

B

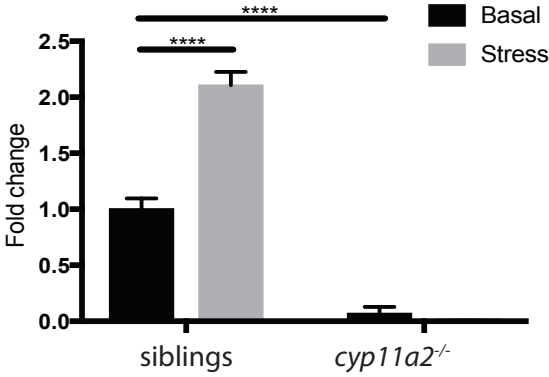
fkbp5
****
****
Basal
Stress
2.5
2.0
1.5
1.0
0.5
0.0
Fold change
siblings
cyp11a2-/-

C

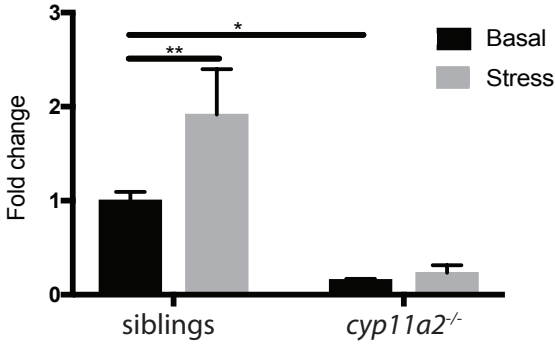
pck1
*
**
Basal
Stress
3
2
1
0
Fold change
siblings
cyp11a2-/-

A

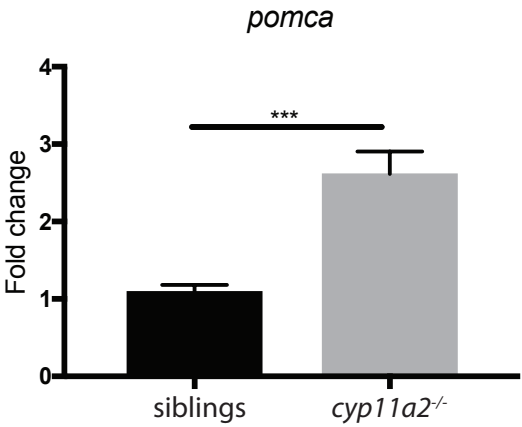
pomca
Fold change
4
3
2
1
0
***
siblings
cyp11a2-/-

B

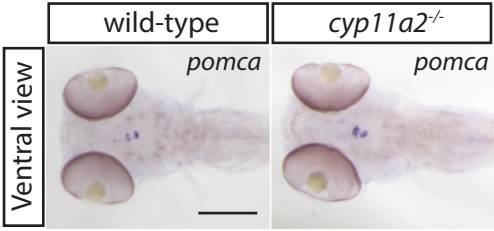
wild-type
cyp11a2-/-
Ventral view
pomca
pomca

A

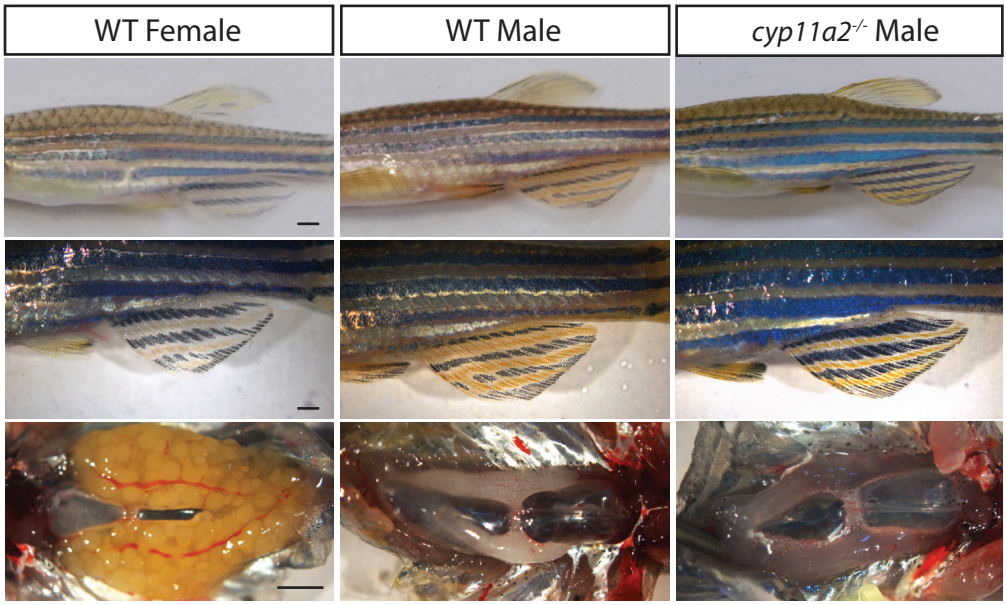
WT Female
WT Male
cyp11a2-/- Male

B

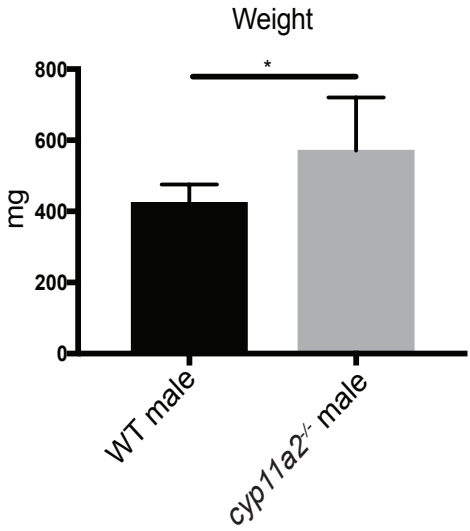
Weight
*
mg
800
600
400
200
0
WT male
cyp11a2-/- male

C

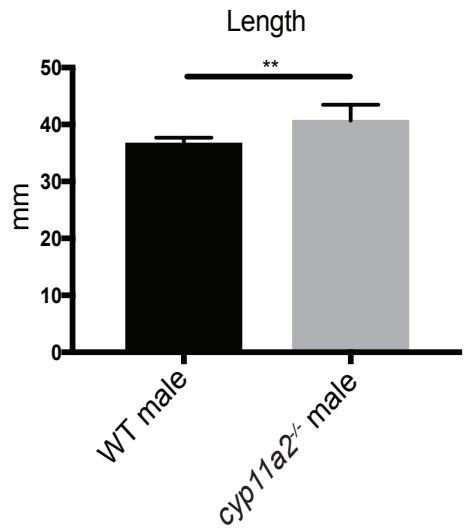
Length
**
mm
50
40
30
20
10
0
WT male
cyp11a2-/- male

D

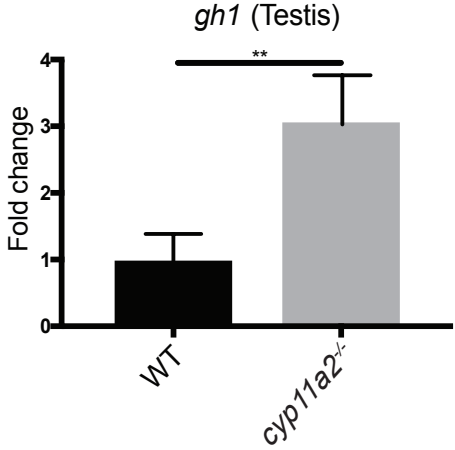
gh1 (Testis)
**
Fold change
4
3
2
1
0
WT
cyp11a2-/-

E

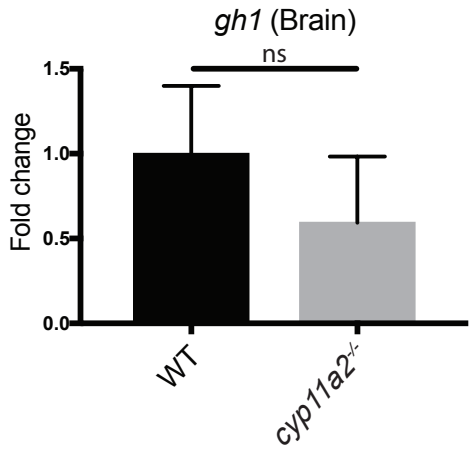
gh1 (Brain)
ns
Fold change
1.5
1.0
0.5
0.0
WT
cyp11a2-/-

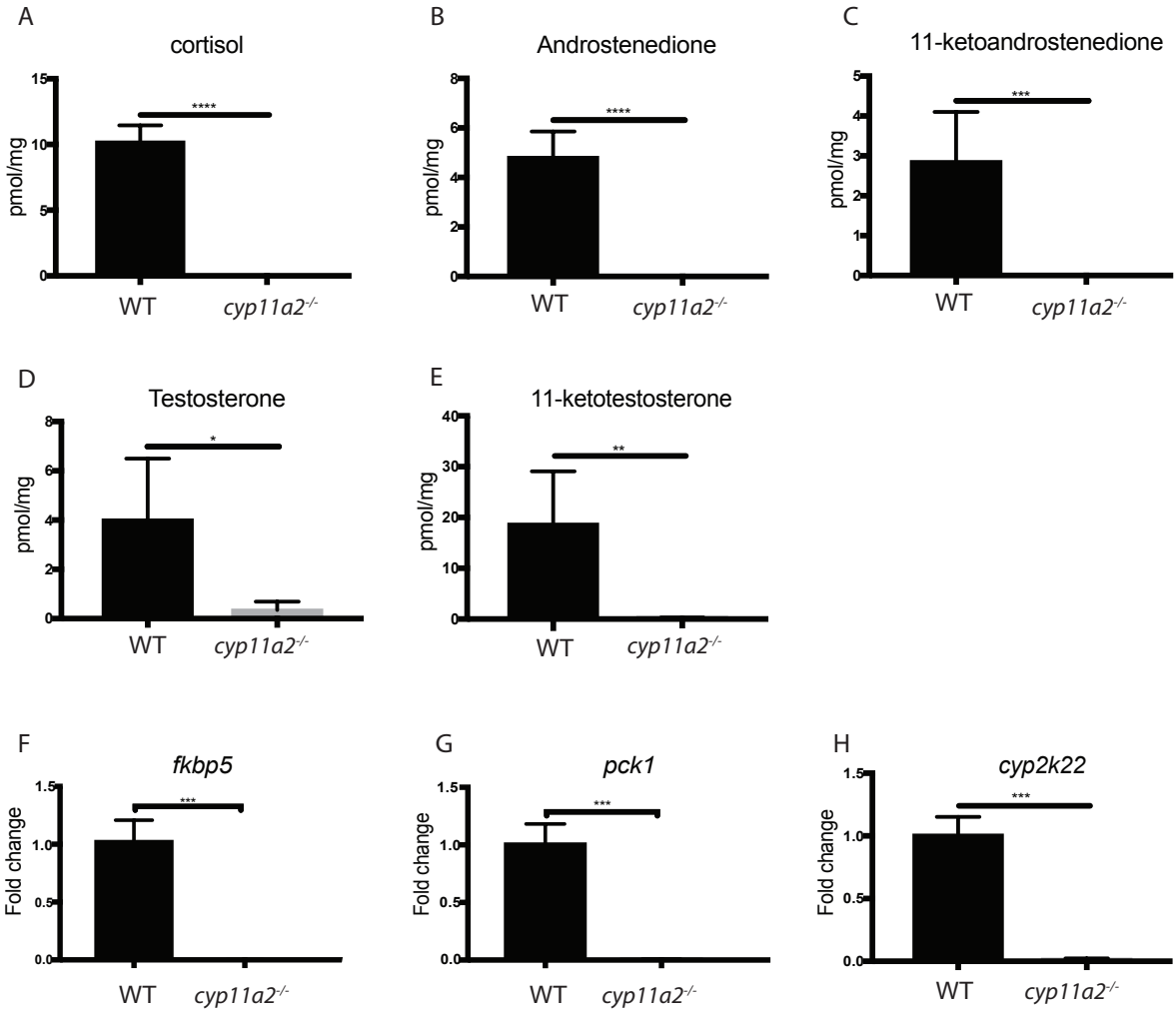
A
cortisol
pmol/mg
15
10
5
0
****
WT
cyp11a2-/-
B
Androstenedione
pmol/mg
8
6
4
2
0
****
WT
cyp11a2-/-
C
11-ketoandrostenedione
pmol/mg
5
4
3
2
1
0
***
WT
cyp11a2-/-
D
Testosterone
pmol/mg
8
6
4
2
0
*
WT
cyp11a2-/-
E
11-ketotestosterone
pmol/mg
40
30
20
10
0
**
WT
cyp11a2-/-
F
fkbp5
Fold change
1.5
1.0
0.5
0.0
***
WT
cyp11a2-/-
G
pck1
Fold change
1.5
1.0
0.5
0.0
***
WT
cyp11a2-/-
H
cyp2k22
Fold change
1.5
1.0
0.5
0.0
***
WT
cyp11a2-/-

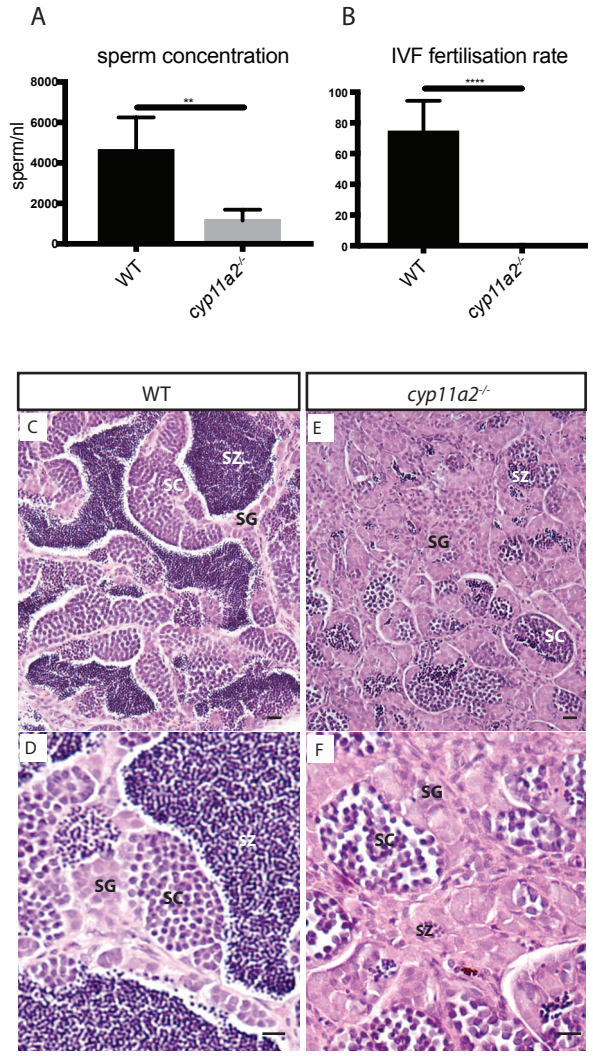
A
sperm concentration
sperm/ml
8000
6000
4000
2000
0
**
WT
cyp11a2-/-
B
IVF fertilisation rate
100
80
60
40
20
0
****
WT
cyp11a2-/-
WT
cyp11a2-/-
C
SZ
SC
SG
D
SZ
SG
SC
E
SZ
SG
SC
F
SG
SC
SZ

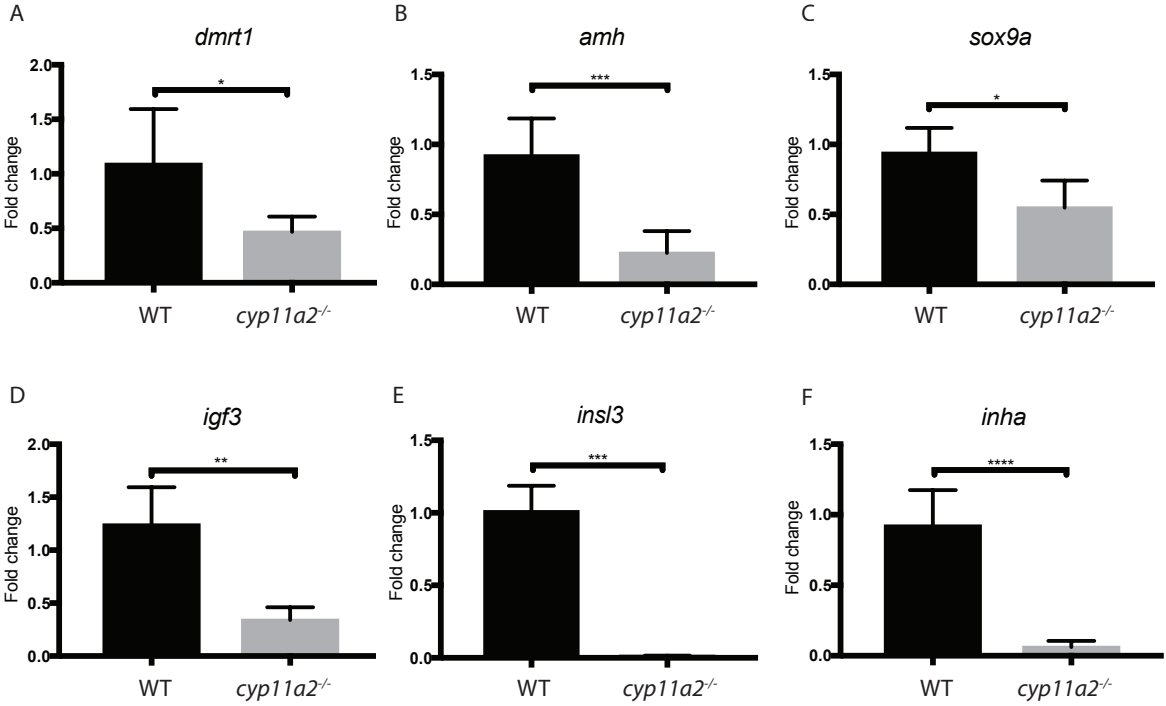
A
dmrt1
Fold change
2.0
1.5
1.0
0.5
0.0
*
WT
cyp11a2-/-
B
amh
Fold change
1.5
1.0
0.5
0.0
***
WT
cyp11a2-/-
C
sox9a
Fold change
1.5
1.0
0.5
0.0
*
WT
cyp11a2-/-
D
igf3
Fold change
2.0
1.5
1.0
0.5
0.0
**
WT
cyp11a2-/-
E
insl3
Fold change
1.5
1.0
0.5
0.0
***
WT
cyp11a2-/-
F
inha
Fold change
1.5
1.0
0.5
0.0
****
WT
cyp11a2-/-

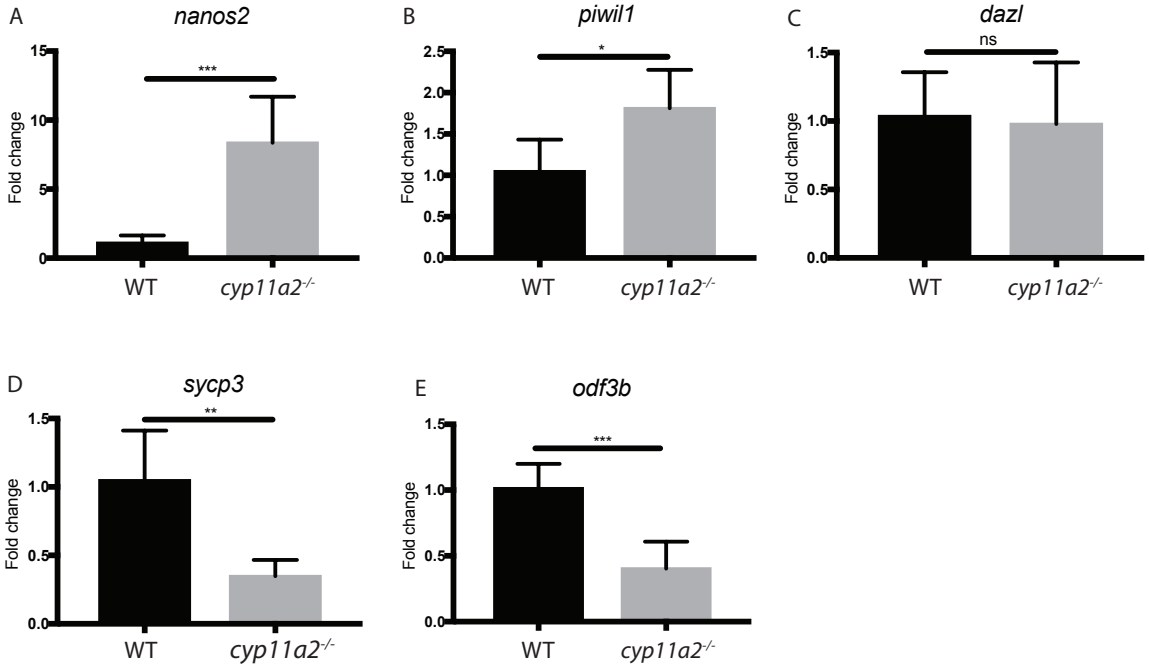
A
nanos2
***
Fold change
15
10
5
0
WT
cyp11a2-/-
B
piwil1
*
Fold change
2.5
2.0
1.5
1.0
0.5
0.0
WT
cyp11a2-/-
C
dazl
ns
Fold change
1.5
1.0
0.5
0.0
WT
cyp11a2-/-
D
sycp3
**
Fold change
1.5
1.0
0.5
0.0
WT
cyp11a2-/-
E
odf3b
***
Fold change
1.5
1.0
0.5
0.0
WT
cyp11a2-/-

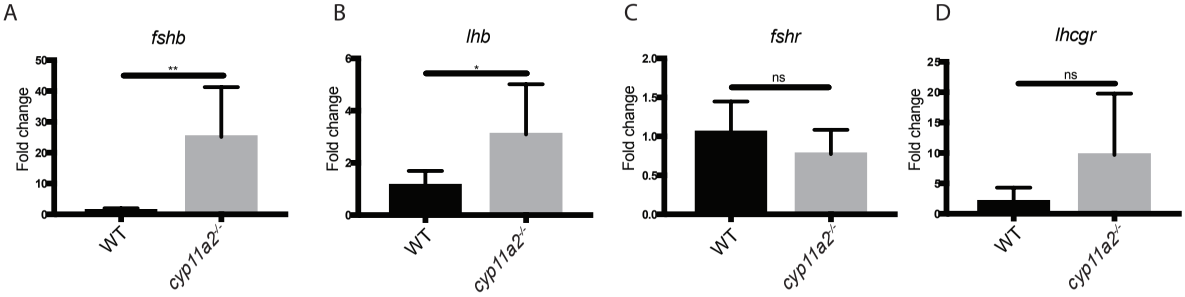
A
fshb
Fold change
50
40
30
20
10
0
**
WT
cyp11a2-/-
B
lhb
Fold change
6
4
2
0
*
WT
cyp11a2-/-
C
fshr
Fold change
2.0
1.5
1.0
0.5
0.0
ns
WT
cyp11a2-/-
D
lhcgr
Fold change
25
20
15
10
5
0
ns
WT
cyp11a2-/-

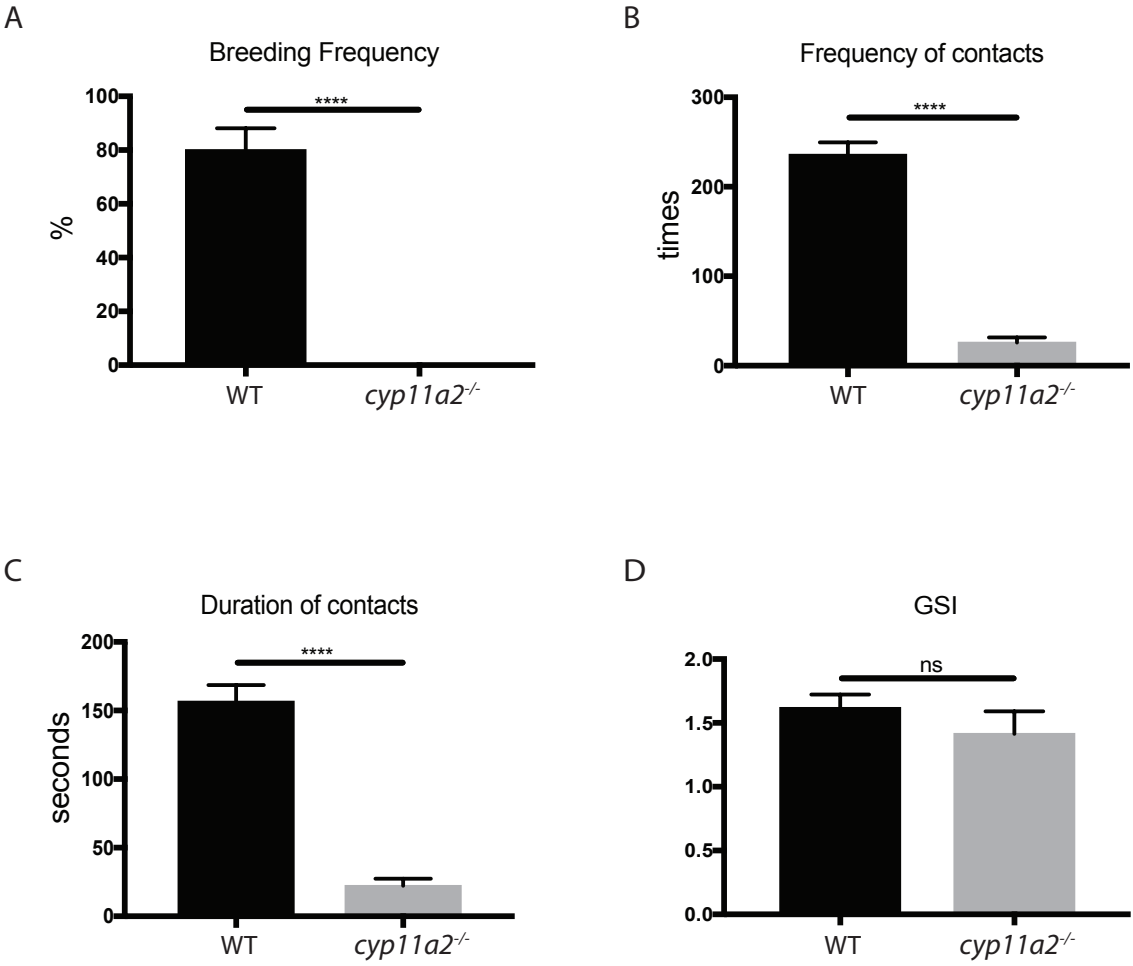
A
Breeding Frequency
%
100
80
60
40
20
0
****
WT
cyp11a2-/-
B
Frequency of contacts
times
300
200
100
0
****
WT
cyp11a2-/-
C
Duration of contacts
seconds
200
150
100
50
0
****
WT
cyp11a2-/-
D
GSI
2.0
1.5
1.0
0.5
0.0
ns
WT
cyp11a2-/-